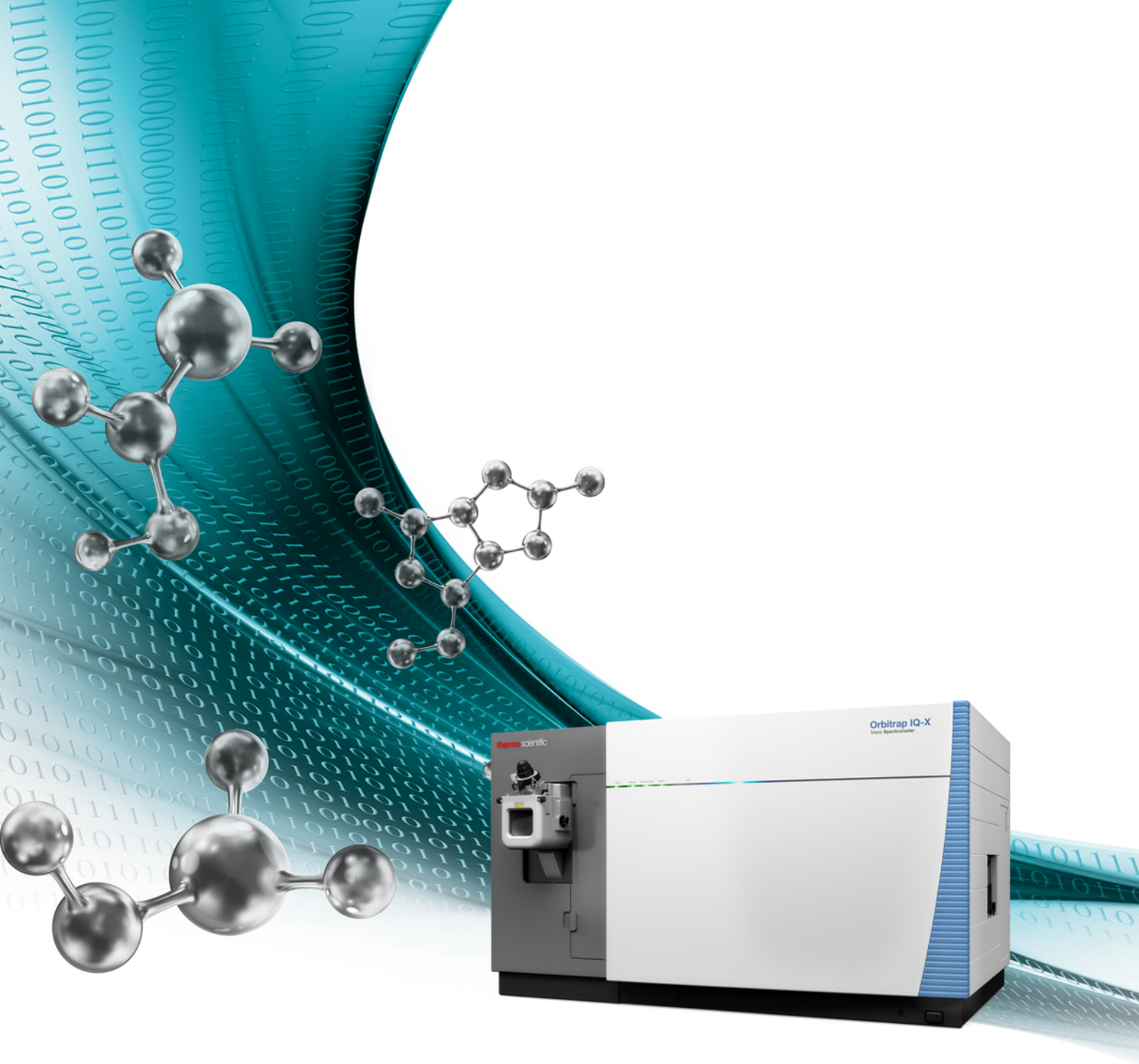

Designed to unravel complex chemical structures

Orbitrap IQ-X Tribrid mass spectrometer

Learn more

thermo scientific

Special issue article

Journal of Applied Toxicology

Received: 19 January 2017, Revised: 4 February 2017, Accepted: 5 February 2017 Published online in Wiley Online Library: 24 May 2017

(wileyonlinelibrary.com) DOI 10.1002/jat.3462

Mechanism of graphene-induced cytotoxicity: Role of endonucleases

Tariq Fahmi[a], La Donna Branch[a], Zeid A. Nima[b], Dae Song Jang[a], Alena V. Savenka[a], Alexandru S. Biris[b] and Alexei G. Basnakian[a,c]*

ABSTRACT: Graphene, a crystalline allotrope or carbon, presents numerous useful properties; however, its toxicity is yet to be determined. One of the most dramatic and irreversible toxic abilities of carbon nanomaterials is the induction of DNA fragmentation produced by endogenous cellular endonucleases. This study demonstrated that pristine graphene exposed to cultured kidney tubular epithelial cells is capable of inducing DNA fragmentation measured by terminal deoxynucleotidyl transferase dUTP nick end labeling (TUNEL) assay, which is usually associated with cell death. TUNEL (cell death) and endonuclease activity measured using a near infrared fluorescence probe was significantly higher in cells containing graphene aggregates detected by Raman spectroscopy. The elevation of TUNEL coincided with the increased abundance of heme oxygenase 1 (HO-1), heat shock protein 90 (HSP90), active caspase-3 and endonucleases (deoxyribonuclease I [DNase I] and endonuclease G [EndoG]), as measured by quantitative immunocytochemistry. Specific inhibitors for HO-1, HSP90, caspase-3, DNase I and EndoG almost completely blocked the DNA fragmentation induced by graphene exposure. Therefore, graphene induces cell death through oxidative injury, caspase-mediated and caspase-independent pathways; and endonucleases DNase I and EndoG are important for graphene toxicity. Inhibition of these pathways may ameliorate cell injury produced by graphene.

Keywords: graphene; DNA fragmentation; endonucleases; DNase I; EndoG; cell death; oxidative injury

Introduction

Graphene is a carbon-based nanomaterial that has extraordinary properties, which promoted its ongoing revolutionary use in different aspects of life (Gulzar *et al*., 2017). At the same time, this raised many questions regarding its biosafety due to potential toxicity during manufacturing, use and spread in the environment (Lalwani *et al*., 2016).

Graphene is only one of a wide variety of carbon nanomaterials. Even though the data on carbon nanomaterials are incomplete, they present significant evidence of toxicity to cells and *in vivo* (Du *et al*., 2013). At least in part, nanomaterial toxicity is caused by the molecular characteristics of the nanomaterial. For example, carbon nanotubes and other fiber materials act as asbestos-like fibers, and graphene and other sheet-shaped materials are expected to act via their damaging sharp, jagged, flat edges (Akhavan & Ghaderi, 2010; Du *et al*., 2013). Nanoparticles have enhanced cell penetration capacity and much larger surface area compared to routine particles, which leads to a greater toxicity. Carbon nanomaterials can penetrate skin (after topical application), lungs (after inhalation), pass blood–tissue barriers after intravenous injections and accumulate in organs (Ahamed *et al*., 2010). Graphene was shown to accumulate in the kidney (Jasim *et al*., 2016), lungs, liver and spleen after intravenous injection (Kanakia *et al*., 2014). Unlike larger particles, nanoparticles are often taken up by the cell's mitochondria and nucleus with the potential of causing damage in DNA (Møller *et al*., 2014). Reactive oxygen species (ROS) are one of the primary mechanisms of nanomaterial toxicity (Lalwani *et al*., 2016; Lam *et al*., 2006; Møller *et al*., 2014; Ou *et al*., 2016). This mechanism causes oxidative stress, inflammation and consequent damage to membranes, proteins and DNA.

The integrity of DNA is very important for cell viability. DNA, being a blueprint of the entire cell and the body, is the last guarantor that damaged cells can recover. DNA is the only molecule in the cell that cannot be resynthesized, it can only be repaired, if damaged. However, the DNA repair capacity of the cell is very limited. Toxic insult by nanomaterials often causes irreparable DNA damage, which is the first step of irreversible cell death. Toxicity of graphene as any nanomaterial to a cell may take various ways. It may start with membrane damage, oxidative injury or apoptosis, but they all come down to DNA fragmentation (Lalwani *et al*., 2016; Ou *et al*., 2016). The cell dies because fragmented DNA cannot be used as a template for new DNA, RNA and proteins, including lipid-metabolizing enzymes. Because of this DNA fragmentation is used as the most reliable *in vitro* and *in vivo* marker of cell death. Most commonly, DNA fragmentation is measured using the terminal deoxynucleotidyl transferase dUTP nick end labeling (TUNEL) assay (Apostolov *et al*., 2009; Liu *et al*., 2017; Singh *et al*., 2013).

The TUNEL assay has several advantages. It measures final, irreversible cell death. The measurement is on an individual cell basis, which is very important for particle toxicity. This measurement does not require the destruction of a cell, such as

*Correspondence to: Alexei G. Basnakian, MD, PhD, DSc Professor, Department of Pharmacology & Toxicology Director, DNA Damage and Toxicology Core Center University of Arkansas for Medical Sciences 4301 West Markham, 638 Little Rock, AR 72205, USA.
E-mail: basnakianalexeig@uams.edu

[a]Department of Pharmacology and Toxicology, University of Arkansas for Medical Science, Little Rock, AR, USA

[b]Center for Integrative Nanotechnology Sciences, University of Arkansas at Little Rock, Little Rock, AR, USA

[c]Central Arkansas Veterans Healthcare System, Little Rock, AR, USA

in the Comet assay (Klein *et al.*, 2008). Instead, TUNEL can be easily combined with immunohistochemistry (Singh *et al.*, 2013). It can be universally applied for all cells and tissues. As opposed to other assays, such as, the annexin V assay (Huerta *et al.*, 2007) that targets apoptosis only, or propidium iodide release (Pick *et al.*, 2004) that is used to measure necrosis, TUNEL is independent of the type of cell death. Many viability and cell death assays can only be applied to suspended or attached cultured cells, such as the MTT assay (Liu *et al.*, 2015) that measures mitochondrial proliferation, or lactic dehydrogenase release assay (Kinard *et al.*, 2001), propidium iodide (Pick *et al.*, 2004), or trypan blue exclusion (Mahmood *et al.*, 2009) assays, which assess plasma membrane leakage, whereas TUNEL assay can be equally applied for both *in vitro* and *in vivo* injury measurements. This offered a great advantage of comparison and translation of data obtained with cultured cells to animal and human studies.

DNA fragmentation can potentially be caused by ROS or even via a direct action of a nanomaterial (for example, by sharp edges of graphene sheets). However, 99% of the time DNA fragmentation is provided by endogenous cellular enzymes traditionally called "apoptotic endonucleases" (Hengartner, 2001). Studies showed that same enzymes participate in other types of cell death, particularly, necrosis (Singh *et al.*, 2013), and prevent the entering of extracellular DNA into the cell (Buzder *et al.*, 2009). Most studied of these endonucleases are deoxyribonuclease I (DNase I) and endonuclease G (EndoG). They are expressed in all cells and tissues, and seem to act simultaneously in cell death (Yin *et al.*, 2007). The role of the endonucleases in graphene and other nanomaterial toxicities has not been identified, partially, because specific inhibitors to study these enzymes were not available. We have recently reported the first specific inhibitors for these endonucleases (Jang *et al.*, 2015a,b), and apply those in the current study.

Therefore, the aim of this study was to determine whether graphene induces DNA fragmentation, and identify the mechanism that causes it. The study was based on the TUNEL assay, which we supplemented with the new approach utilizing the near infrared fluorescent (NIRF) probe (Jang *et al.*, 2015a,b) to measure the endonuclease activity intravitally. These two methods complemented each other because both are based on the measurement of endonuclease-mediated DNA fragmentation.

Materials and methods

Chemicals

Pristine (non-modified) graphene was obtained from the National Center for Toxicological Research (Jefferson, AR, USA). Even though graphene was not modified, it might have been spontaneously weakly oxidized due to processing and storage. Tin protoporphyrin IX dichloride (Santa Cruz, CA, USA) was used as heme oxygenase-1 (HO-1) inhibitor at final concentration of 10 μM. Ac-DEVD-CHO (EMD Millipore, Darmstadt, Germany) (50 μM) was used to inhibit caspase-3. Heatshock protein (HSP) 90 inhibitor AT13387 from MedChemExpress (Monmouth Junction, NJ, USA) was used at 20 nM. DNase I chemical inhibitors JR-132 and IG-17 (100 μM each) and EndoG inhibitors PNR-3-82 and PNR-3-80 (50 μM each) were used as previously described (Jang *et al.*, 2015a,b). If not specifically indicated, all other reagents were from Sigma-Aldrich (St. Louis, MO, USA).

Cell culture and graphene exposure

Kidney cells were used in these studies because the kidney is a common target for graphene and other nanomaterials (Jasim *et al.*, 2016). Normal rat tubular epithelial NRK-52E cells (ATCC, Manassas, VA, USA) were grown in Dulbecco's modified Eagle's medium (ATCC) supplemented with 5% fetal bovine sera. Cells were cultured at 5% CO_2/95% air in a humidified atmosphere at 37°C, fed at intervals of 48–72 h, and used within 1 day after confluence. Cells were exposed to graphene at varying concentrations for 24–48 h. Enzyme inhibitors, if applied, were added for 2 h before exposure to graphene.

Intravital endonuclease activity measurement

The total DNase (DNA endonuclease) activity in live cells was measured using the DNase activity NIRF probe AB259.3 as described previously (Jang *et al.*, 2015a,b). The probe is a cell-permeable DNA hairpin oligonucleotide labeled with Cy5.5 fluorophores at both ends, with the structure of 5′[Cy5.5]AACACT CCGATGAGTGTAGAATGT[Cy5.5][3P]-3′. After annealing of the hairpin, the fluorophores are in close proximity and they quench each other. A degradation of the probe by endonucleases separates them, which increases the fluorescence signal.

Immunocytochemistry, TUNEL and image analyses

The cells were washed twice with phosphate-buffered saline, fixed with 4% paraformaldehyde and immunostained with primary antibody in dilution buffer (0.5% bovine serum albumin, 0.05% Tween-20, phosphate-buffered saline). The primary antibodies (Table 1, Supporting Information) were detected with secondary IgG-AlexaFluor 488 or IgG-AlexaFluor 594 conjugates (Invitrogen, Carlsbad, CA, USA). Control stainings were performed by substituting the primary antibody with dilution buffer. In some experiments, cells were additionally stained with TUNEL assay using the In Situ Cell Death Detection Kit (Roche Diagnostics, Indianapolis, IN, USA) according to the manufacturer's protocol. After staining, cells were counterstained with 4′,6-diamidino-2-phenylindol (DAPI) to visualize cell nuclei, mounted under cover slips with Prolong® Antifade kit (Invitrogen) and acquired using the Olympus IX-81 inverted microscope (Olympus America, Center Valley, PA, USA) equipped with Hamamatsu ORCA-ER monochrome camera (Hamamatsu Photonics K.K., Hamamatsu City, Japan). Image analysis was performed using SlideBook 4.2 software. For quantification, 10 independent fields of view were collected per each well, and mean optical density (MOD) was recorded for AlexaFluor 488 or 594 channel. The data were presented as averages of MOD per field of view for each channel.

Raman microscopy

Raman microscopy/spectroscopy was used for the identification and localization of graphene in the cells. Cells were grown and fixed as described for TUNEL. The Raman data were collected with a Horiba Jobin Yvon LabRam HR800 spectrometer (New Jersey, USA) equipped with 600 lines mm^{-1} gratings and a Peltier-cooled CCD camera. The overall spectral resolution is around 1 cm^{-1}. Raman spectrometer was calibrated before the studies by using a silicon wafer based on the silicon specific peak at 521 cm^{-1}. The signal was collected in the backscattering geometry by a confocal Raman system equipped with an Olympus BX51

Journal of Applied Toxicology

microscope with 10, 50 and 100× objectives. All the measurements were performed with the 100X objective. The spectrometer was also connected to an automated stage which is capable of providing software controlled 3D(*x,y,z*) spatial scanning with a variable step size. The laser excitation wavelengths was 785 nm, and a power at the sample surface of about 2 mW.

Results

Graphene induces DNA fragmentation in cultured cells

Rat renal tubular epithelial NRK-52E cells were exposed to varying concentrations of graphene for 24 h. Graphene aggregates were visualized using phase contrast microscopy, DNA fragmentation indicating cell death was detected and then measured using the TUNEL assay (Fig. 1A). Low concentrations of graphene, up to 25 μg ml^{-1}, were found not to result in any elevation of DNA fragmentation above vehicle control samples, and thus were not considered cytotoxic (Fig. 1B). However, starting from 50 μg ml^{-1}, the elevation of TUNEL over vehicle control was statistically significant, indicating the cytotoxicity.

We next examined whether activity NIRF probe AB289.3 will be able to determine increase of DNA endonuclease activity during cell death, which would explain the increase of TUNEL. The results showed that NRK-52E cells exposed to graphene (50 μg ml^{-1}) for 24 h had a significantly higher NIRF signal indicating that the increase of endonuclease activity compared to untreated cells (Fig. 1C; Supporting Information, Fig. S1A–C). At the same time, the intensity of the DAPI staining of polymeric nuclear DNA was significantly decreased (Fig. 1D). These data suggested that fragmentation of cellular DNA was induced by exposure to graphene.

Increase of graphene clusters in cell is associated with increase of cytotoxicity

Being a particulate matter, graphene is not distributed equally between cells. Thus, it is important detecting it in the cells, and colocalizing it with cells showing TUNEL positivity as the evidence of injury. We used phase-contract microscopy to identify graphene particles, and applied more precise Raman spectroscopy to measure the presence of graphene in the cells. Our experiments showed that cells exposed to graphene at 50 μg ml^{-1} had higher integrated Raman intensity than untreated or control (vehicle-treated) cells; and cells with graphene accumulation had higher integrated Raman intensity than cells without graphene accumulation (Supporting Information, Fig. S2A). These data

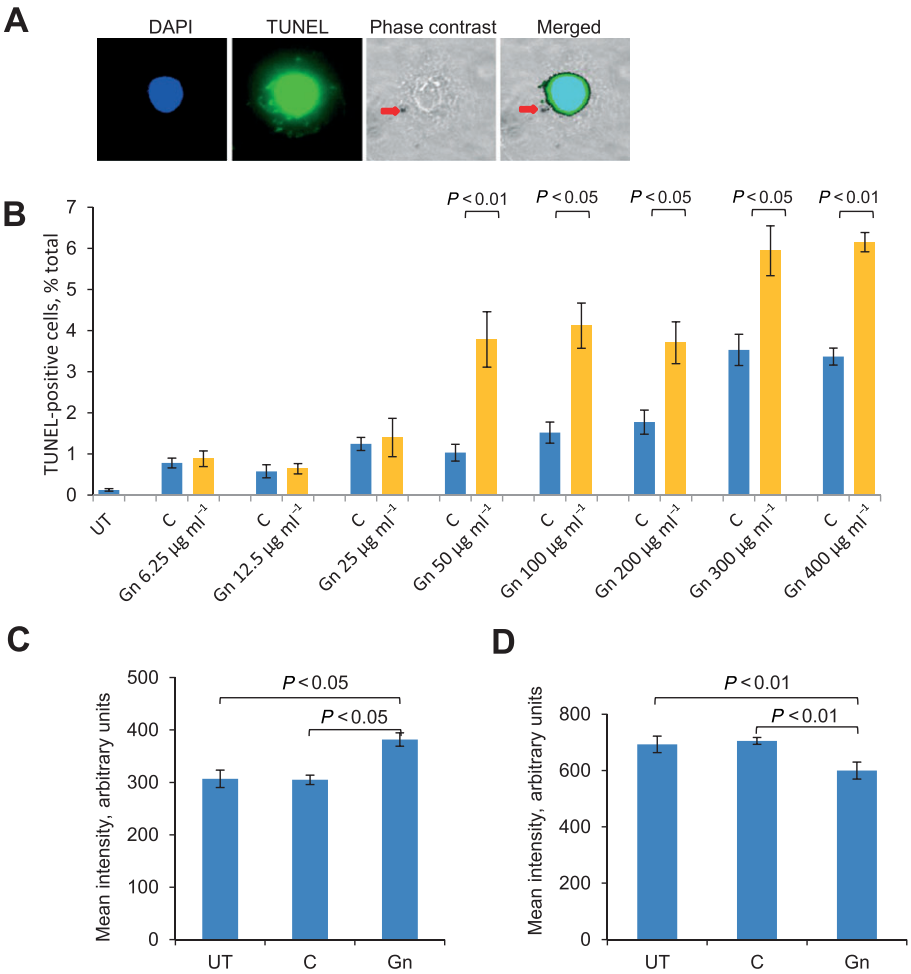

Figure 1. Measurement of graphene toxicity in renal tubular epithelial cells. (A) Nuclear TUNEL staining (green) indicative of DNA fragmentation and cell death is located in the cell that contains a graphene cluster (shown by red arrow). (B) TUNEL assay measurement of graphene cytotoxicity at varying concentrations. (C) Quantification of DNase activity near infrared fluorescence. (D) Nuclear polymeric DNA staining by DAPI in NRK-52E cells. C, control vehicle-treated cells; Gn, cells exposed to graphene; UT, untreated cells.

confirmed that graphene has been delivered to the cells either in the form of single particles or aggregates.

To determine whether TUNEL positivity is associated with (and caused by) graphene, NRK-52E cells exposed to graphene (50 μg ml^{-1}) for 24 h were stained for TUNEL and then sorted by flow cytometry to separate TUNEL-positive ($TUNEL^+$) and TUNEL-negative ($TUNEL^-$) cells. The percentage of $TUNEL^+$ cells was 3.8% (Supporting Information, Fig. S2B), which is very close to the percentage determined above in fixed attached cells. From the graphene-treated group, 10 cells from each $TUNEL^+$ and $TUNEL^-$ sorted cells were subjected to Raman spectroscopy to determine if the nanomaterial can be associated with TUNEL-positivity (DNA fragmentation and cell death). The results showed that $TUNEL^+$ cells had a significantly higher integrated Raman intensity than $TUNEL^-$ cells, which suggested that the $TUNEL^+$ cells had more graphene than $TUNEL^-$ cells (Fig. 2A). Furthermore, the DNA endonuclease activity measured in live cells using the NIRF probe mean intensity showed that the latter directly correlated with the intracellular graphene's mean intensity (Fig. 2B), while DAPI mean intensity (the amount of polymeric DNA) inversely correlated with the graphene mean intensity (Fig. 2C). Taken together, these data suggest that intracellular graphene induced elevation of DNA endonuclease activity, and caused DNA fragmentation and cell death.

Graphene induces heme oxygenase-1 and apoptotic endonucleases, and activates caspase-3

Our further experiment was aimed to determine the cause of the elevation of DNA endonuclease activity. In addition to testing several key endonucleases, we chose to test the involvement of oxidative injury, as a known inducer of endonucleases (Basnakian *et al.*, 2002; Ishihara & Shimamoto, 2006), and HSPs, known as important regulators of apoptosis (Rerole *et al.*, 2011).

NRK-52E cells were exposed to graphene (50 μg ml^{-1}) for 24 h, then fixed and immunostained. First, the immunocytochemistry (ICC) was performed for three markers of oxidative stress: HO-1, inducible nitric oxide synthase, and oxoguanine glycosylase (OGG-1). The results showed that HO-1 is significantly induced in graphene-treated cells compared to untreated and control cells (Fig. 3A). At the same time, inducible nitric oxide synthase and OGG-1 did not show any statistically significance induction by graphene above control (Supporting Information, Fig. S2A,B). Similar to OGG-1, which is a DNA repair enzyme, another DNA repair enzyme of the DNA base excision pathway, apurinic/apyrimidinic endonuclease-1, also did not show any induction, and was even reduced by graphene exposure (Supporting Information, Fig. S3C). Among HSPs, qICC of HSP40 and HSP60 showed no significant difference between the groups (Supporting Information, Fig. S3D,E) while HSP70 is slightly elevated in graphene-treated cells but it did not reach the level of significance (Supporting Information, Fig. S3F). On the contrary, HSP90 was significantly induced by graphene exposure (Fig. 3B).

The comparison of two apoptotic pathway markers, EndoG, a marker of caspase-independent apoptosis (Singh *et al.*, 2013), and active caspase-3 that is a mechanistic marker of caspase-mediated apoptosis showed that both of them were significantly elevated in NRK-52 cells exposed to graphene (Fig. 3C,D). These results suggested that both caspase-mediated and caspase-independent pathways were involved in the DNA fragmentation in NRK52E cells exposed to graphene.

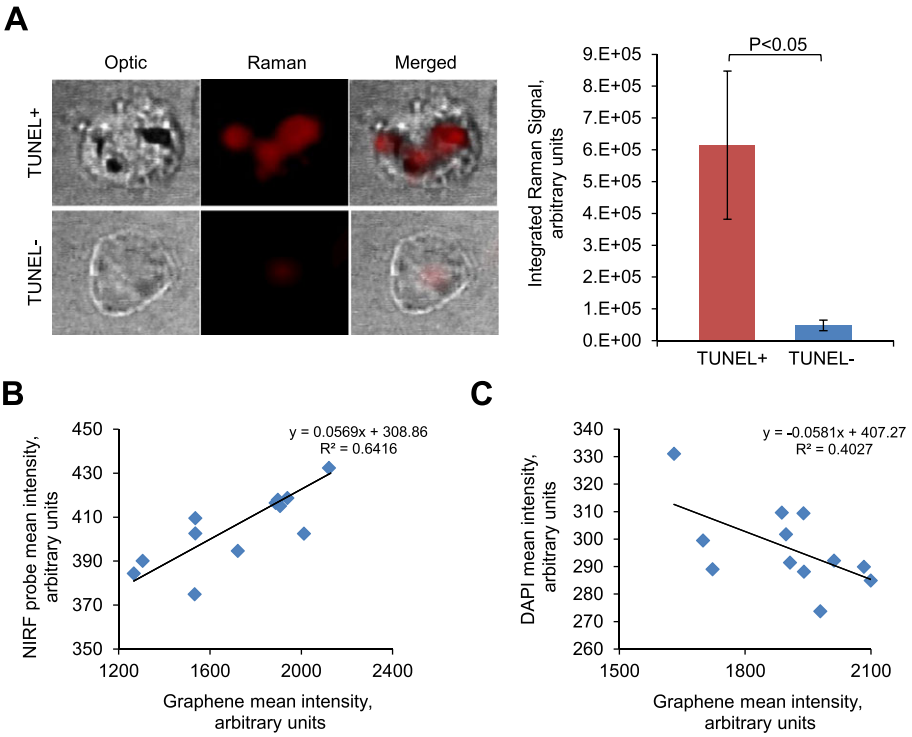

Figure 2. Cells containing graphene clusters have more DNA fragmentation. (A) Representative 2D Raman maps developed based on the graphene specific signature (left). Integrated Raman spectroscopy signal is higher in $TUNEL^+$ versus $TUNEL^-$ cells (right). (B) DNA endonuclease activity measured by NIRF probe signal directly correlates with graphene quantity (mean intensity). (C) DNA quantity measure by DAPI mean intensity reversely correlates with graphene quantity (mean intensity), which indicates degradation and removal of some DNA. NIRF, near infrared fluorescence.

Journal of Applied Toxicology

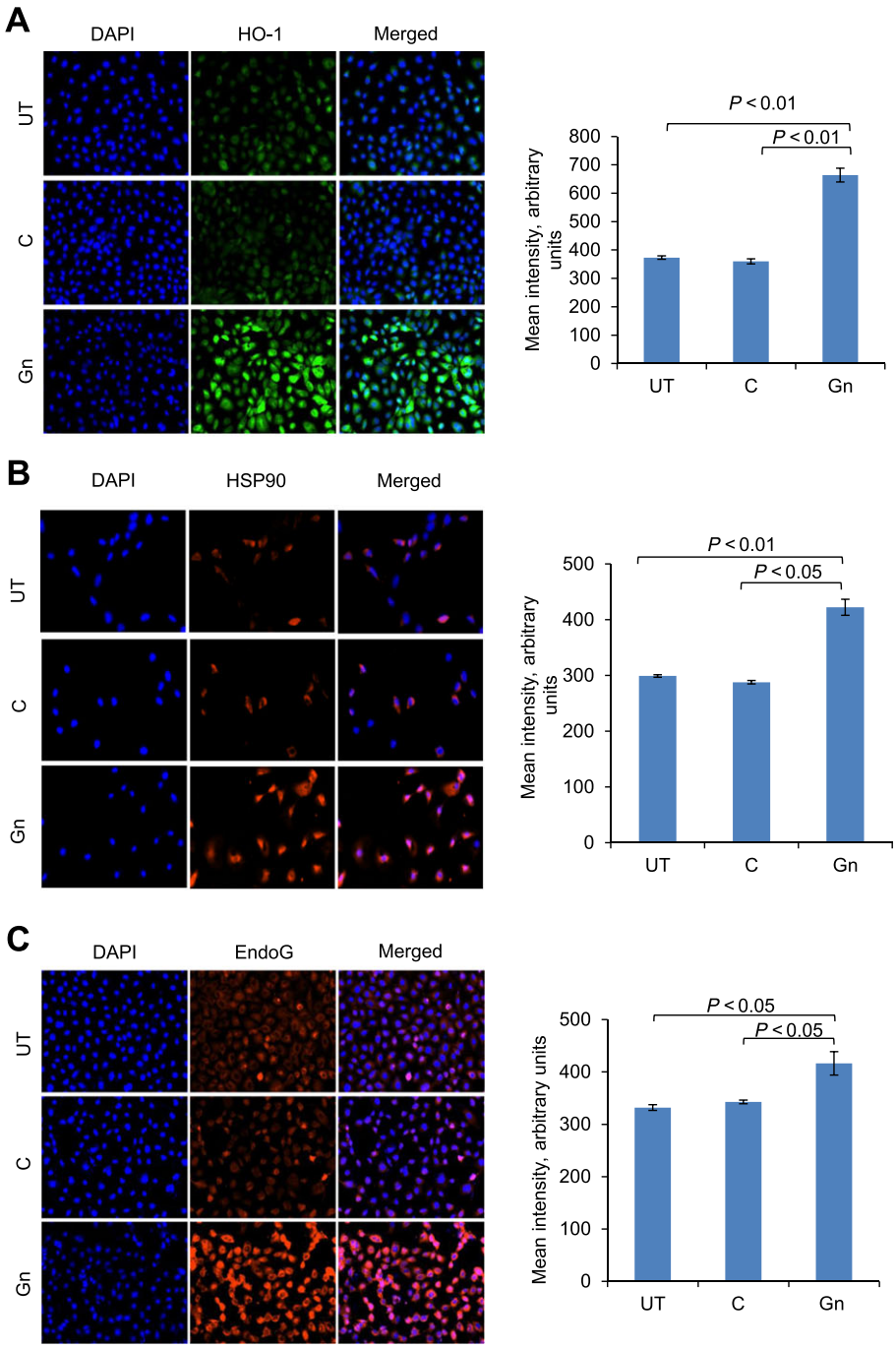

Figure 3. Immunocytochemical measurement of oxidative and apoptotic markers affected by graphene (50 μg ml^{-1}) exposure of NRK-52E cells. (A) Graphene induces HO-1 (green staining). (B–D) HSP90, EndoG and active caspase-3 immunostaining (red color) and quantification of their mean intensities, respectively, in NRK-52E cells. (E,F) Quantification of DNase I and CAD mean intensities, respectively, in NRK-52E cells exposed to graphene. C, control vehicle-treated cells; Gn, cells exposed to graphene; HO-1, heme-oxygenase-1; HSP90, heatshock protein 90; UT, untreated cells.

We further assessed the involvement of other endonucleases, such as DNase I and caspase-activated DNase, and found that both of them were significantly elevated in NRK-52E cells treated with graphene (Fig. 3E,F). These results suggested that apoptotic endonucleases seem to be involved in graphene cytotoxicity. However, there was still a need for cause–effect relationships between graphene toxicity and the individual molecules to be established.

Alleviation of the graphene cytotoxicity by chemical inhibitors

To test the cause–effect relationships between graphene cytotoxicity and the individual markers, specific inhibitors were applied. Before graphene, NRK-52E cells were exposed to the HO-1 chemical inhibitor protoporphyrin IX, caspase-3 inhibitor Ac-DEVD, HSP90 inhibitor AT13387, DNase I inhibitors JR-132 and IG-17, or EndoG inhibitors PNR-3-80 and PNR-3-82. Two hours later,

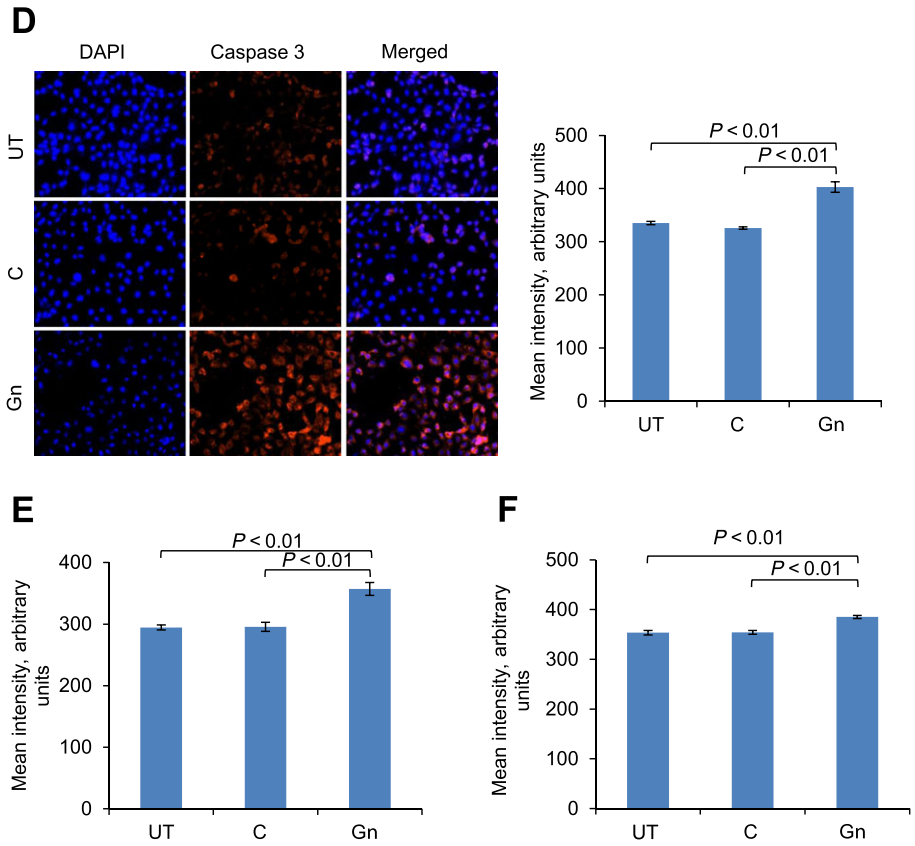

Figure 3. *Continued*

graphene was added to 50 μg ml^{-1} for 48 h. TUNEL assay showed that all these inhibitors were able to reduce cell death significantly, more than three-fold compared to cells treated with graphene only (Fig. 4). This observation confirmed the mechanistic contribution of HO-1, caspase 3, HSP90, DNase I and EndoG in the graphene toxicity.

Discussion

Toxicology studies of every new nanomaterial are notoriously incomplete, and its potential toxicity is always a concern. The reasons for this are many: invention of new nanomaterials are way ahead of the toxicity studies, which take a long time to

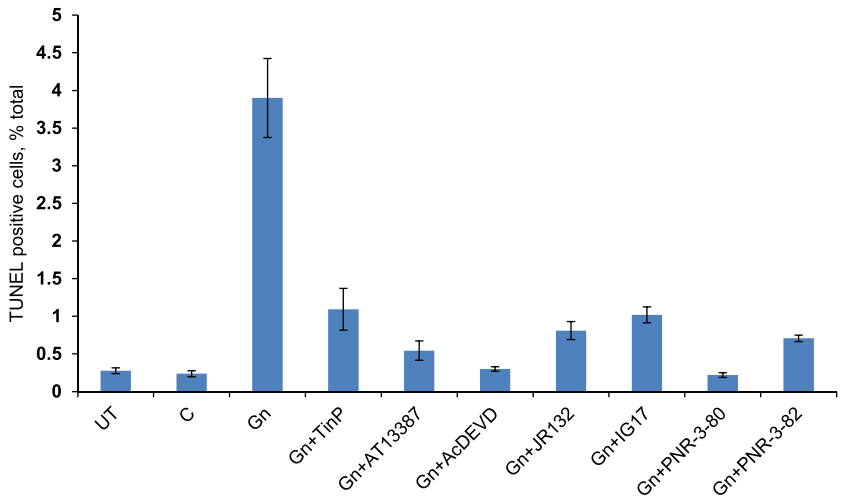

Figure 4. Alleviation of graphene toxicity by using chemical inhibitors after 48 h exposure of NRK-52E cells with graphene (50 μg ml^{-1}). Quantification of TUNEL-positive cells in NRK-52E cells treated with graphene in the presence of chemical inhibitors for HO-1, HSP90, caspase 3, DNase I and EndoG ($p < 0.01$ for all bars vs. Gn).

complete; the methods used for routine toxicity analyses may not be satisfactory for nanomaterial toxicity; and toxicity patterns of the new nanomaterials are unknown. Toxicology is usually based on the concepts of determining the known toxic effects. When the effects are unknown, the study becomes unfocused and may end up with getting false-negative results. In this regard, using DNA fragmentation gives the advantage of a universally applicable method to assess any cellular damage independent of the mechanism. Endonuclease-mediated DNA damage is known to be the last step in cell death, after which cell death becomes irreversible. Cell death mediated by endonucleases can occur by an immediate cause or/and because of apoptosis and all other types of irreversible cell death during tissue injury. It is produced by different enzymes, including DNase I, caspase-activated DNase, EndoG and other DNA-degrading enzymes enzymes, which act simultaneously during cell death. Apoptotic endonucleases are the enzymes that are weakly cytotoxic themselves, but they universally promote the cytotoxicity of various agents, including nanomaterials. Induction and nuclear import of the endonucleases is attributed to an irreversible stage of cell death manifested with the fragmentation of DNA (Hengartner, 2001).

In this study, we demonstrated that pristine graphene exposed to cultured kidney tubular epithelial cells is capable of inducing DNA fragmentation measured by TUNEL assay commonly associated with cell death. TUNEL (cell death) and endonuclease activity measured using a NIRF probe was significantly higher in cells containing graphene aggregates detected by Raman spectroscopy. The elevation of TUNEL coincided with the increased abundance of HO-1, HSP90, active caspase-3, DNase I and EndoG as measured by ICC. Specific inhibitors for HO-1, HSP90, caspase-3, DNase I and EndoG almost completely blocked the DNA fragmentation induced by graphene exposure. Therefore, graphene induces cell death through oxidative injury, caspase-mediated and caspase-independent pathways; and endonucleases DNase I and EndoG are important for graphene toxicity.

Knowing these pathways may help in studies of graphene, and, potentially, other carbon nanomaterial toxicities. Our data regarding the anti-graphene toxicity activity of DNase I and EndoG inhibitors are the first indicating the mechanistic role of these apoptotic endonucleases in graphene toxicity. These inhibitors could be used in future to ameliorate graphene toxicity in different systems.

Some studies based on the *in vitro* toxicity of graphene reasonably hypothesized that the measured biological findings will actually vary across the material family based on the number of layers, lateral dimensions, mechanical stiffness, hydrophobic/hydrophilic characteristics, hydrophobicity, surface chemical functionalization, charges, coating and dose (Sanchez *et al*. 2012; Yang *et al*., 2013). The latter, which is also at the basis of the entire toxicology discipline, was confirmed by the current report. Our study also supported previous observation by Zhang *et al*. (2010) regarding activation of caspase-3 by graphene, and the involvement of ROS in graphene toxicity (Nedosekin *et al*., 2014; Pogacean *et al*., 2014; Wilczek *et al*., 2015). Several reports used the advantage of TUNEL to demonstrate graphene toxicity (Liu *et al*., 2017; Shim *et al*., 2014). However, we could not find any study in the literature that would involve identification of individual endonuclease producing TUNEL-like DNA fragmentation. It is important that we were able to associate the presence of graphene agglomerates in the cells with TUNEL, thus linking these two events into an apparent consequence events. Identification of individual nanoparticles often presents a problem because the size of the nanomaterials varies. Carbon-based and other nanomaterials are often heterogeneous, impure and prone to agglomeration (Lim *et al*., 2012). Carbon nanotubes and other nanomaterials are able to cross plasma membranes, enter cells and accumulate in the cytoplasm causing cell death (Dong *et al*., 2008; Tian *et al*., 2006). The conglomerates can form before, during and after the cell consumption of the nanomaterials. Studies show that carbon-based nanomaterials can produce oxidative stress and inflammation (Kim *et al*., 2010; Lam *et al*., 2006), both of which would strongly contribute to activation of endonucleases causing irreversible cell death.

In conclusion, our study, for the first time, identified apoptotic endonucleases as one of the key mechanisms of graphene-induced cytotoxicity, and demonstrated that applying endonuclease inhibitors may be effective in the amelioration of graphene toxicity *in vitro*. Future studies may test whether this approach is applicable *in vivo*.

Acknowledgments

This study was supported by Food and Drug Administration/Arkansas Research Alliance award HHSF223201210189C, National Institutes of Health grant P20 GM109005 and VA Merit Review grant I01 BX002425.

Conflict of interest

The authors did not report any conflict of interest.

References

Ahamed M, Alsalhi MS, Siddiqui MK. 2010. Silver nanoparticle applications and human health. *Clin. Chim. Acta* **411**: 1841–1848.

Akhavan O, Ghaderi E. 2010. Toxicity of graphene and graphene oxide nanowalls against bacteria. *ACS Nano* **4**: 5731–5736.

Apostolov EO, Soultanova I, Savenka A, Bagandov OO, Yin X, Stewart AG, Walker RB, Basnakian AG. 2009. Deoxyribonuclease I is essential for DNA fragmentation induced by gamma radiation in mice. *Radiat. Res.* **172**: 481–492.

Basnakian AG, Kaushal GP, Shah SV. 2002. Apoptotic pathways of oxidative damage to renal tubular epithelial cells. *Antioxid. Redox Signal.* **4**: 915–924.

Buzder T, Yin X, Wang X, Banfalvi G, Basnakian AG. 2009. Uptake of foreign nucleic acids in kidney tubular epithelial cells deficient in proapoptotic endonucleases. *DNA Cell Biol.* **28**: 435–442.

Dong L, Joseph KL, Witkowski CM, Craig MM. 2008. Cytotoxicity of single-walled carbon nanotubes suspended in various surfactants. *Nanotechnology* **19**: 255702.

Du J, Wang S, You H, Zhao X. 2013. Understanding the toxicity of carbon nanotubes in the environment is crucial to the control of nanomaterials in producing and processing and the assessment of health risk for human: a review. *Environ. Toxicol. Pharmacol.* **36**: 451–462.

Gulzar A, Yang P, He F, Xu J, Yang D, Xu L, Jan MO. 2017. Bioapplications of graphene constructed functional nanomaterials. *Chem. Biol. Interact.* **262**: 69–89.

Hengartner MO. 2001. Apoptosis. DNA destroyers. *Nature* **412**(27): 29.

Huerta S, Goulet EJ, Huerta-Yepez S, Livingston EH. 2007. Screening and detection of apoptosis. *J. Surg. Res.* **139**: 143–156.

Ishihara Y, Shimamoto N. 2006. Involvement of endonuclease G in nucleosomal DNA fragmentation under sustained endogenous oxidative stress. *J. Biol. Chem.* **281**(10): 6726–6733.

Jang DS, Penthala NR, Apostolov EO, Wang X, Crooks PA, Basnakian AG. 2015a. Novel cytoprotective inhibitors for apoptotic endonuclease G. *DNA Cell Biol.* **34**: 92–100.

Jang DS, Penthala NR, Apostolov EO, Wang X, Fahmi T, Crooks PA, Basnakian AG. 2015b. Novel high-throughput deoxyribonuclease 1 assay. *J. Biomol. Screen.* **20**: 202–211.

Jasim DA, Murphy S, Newman L, Mironov A, Prestat E, McCaffrey J, Menard-Moyon C, Rodrigues AF, Bianco A, Haigh S, Lennon R, Kostarelos K. 2016. The effects of extensive glomerular filtration of thin graphene oxide sheets on kidney physiology. *ACS Nano* **10**: 10753–10767.

Kanakia S, Toussaint JD, Mullick Chowdhury S, Tembulkar T, Lee S, Jiang YP, Lin RZ, Shroyer KR, Moore W, Sitharaman B. 2014. Dose ranging, expanded acute toxicity and safety pharmacology studies for intravenously administered functionalized graphene nanoparticle formulations. *Biomaterials* **35**: 7022–7031.

Kim JE, Lim HT, Minai-Tehrani A, Kwon JT, Shin JY, Woo CG, Choi M, Baek J, Jeong DH, Ha YC, Chae CH, Song KS, Ahn KH, Lee JH, Sung HJ, Yu IJ, Beck GR, Jr, Cho MH. 2010. Toxicity and clearance of intratracheally administered multiwalled carbon nanotubes from murine lung. *J. Toxicol. Environ. Health A* **73**: 1530–1543.

Kinard F, Jaworski K, Sergent-Engelen T, Goldstein D, Van Veldhoven PP, Holvoet P, Trouet A, Schneider YJ, Remacle C. 2001. Smooth muscle cells influence monocyte response to LDL as well as their adhesion and transmigration in a coculture model of the arterial wall. *J. Vasc. Res.* **38**: 479–491.

Klein P, Cirioni O, Giacometti A, Scalise G. 2008. In vitro and in vivo activity of aurintricarboxylic acid preparations against *Cryptosporidium parvum*. *J. Antimicrob. Chemother.* **62**: 1101–1104.

Lalwani G, D'Agati M, Khan AM, Sitharaman B. 2016. Toxicology of graphene-based nanomaterials. *Adv. Drug Deliv. Rev.* **105**: 109–144.

Lam CW, James JT, McCluskey R, Arepalli S, Hunter RL. 2006. A review of carbon nanotube toxicity and assessment of potential occupational and environmental health risks. *Crit. Rev. Toxicol.* **36**: 189–217.

Lim CH, Kang M, Han JH, Yang JS. 2012. Effect of agglomeration on the toxicity of nano-sized carbon black in Sprague-Dawley Rats. *Environ. Health Toxicol.* **27** e2012015.

Liu F, Mahmood M, Xu Y, Watanabe F, Biris AS, Hansen DK, Inselman A, Casciano D, Patterson TA, Paule MG, Slikker W, Jr, Wang C. 2015. Effects of silver nanoparticles on human and rat embryonic neural stem cells. *Front. Neurosci.* **9**: 115.

Liu J, Liu K, Feng L, Liu Z, Xu L. 2017. Comparison of nanomedicine-based chemotherapy, photodynamic therapy and photothermal therapy using reduced graphene oxide for the model system. *Biomater. Sci.* **5**(2): 331–340.

Mahmood M, Karmakar A, Fejleh A, Mocan T, Iancu C, Mocan L, Iancu DT, Xu Y, Dervishi E, Li Z, Biris AR, Agarwal R, Ali N, Galanzha EI, Biris AS, Zharov VP. 2009. Synergistic enhancement of cancer therapy using a combination of carbon nanotubes and anti-tumor drug. *Nanomedicine (Lond.)* **4**: 883–893.

Møller P, Folkmann JK, Danielsen PH, Jantzen K, Loft S. 2014. Oxidative stress generated damage to DNA by gastrointestinal exposure to insoluble particles. *Curr. Mol. Med.* **12**: 732–745.

Nedosekin DA, Galanzha EI, Dervishi E, Biris AS, Zharov VP. 2014. Super-resolution nonlinear photothermal microscopy. *Small* **10**: 135–142.

Ou L, Song B, Liang H, Liu J, Feng X, Deng B, Sun T, Shao L. 2016. Toxicity of graphene-family nanoparticles: a general review of the origins and mechanisms. *Part. Fibre Toxicol.* **13**: 57.

Pick N, Cameron S, Arad D, Av-Gay Y. 2004. Screening of compounds toxicity against human monocytic cell line-THP-1 by flow cytometry. *Biol. Proc. Online* **6**: 220–225.

Pogacean F, Biris AR, Coros M, Lazar MD, Watanabe F, Kannarpady GK, Al Said SA, Biris AS, Pruneanu S. 2014. Direct electrochemical oxidation of S-captopril using gold electrodes modified with graphene-AuAg nanocomposites. *Int. J. Nanomedicine* **9**: 1111–1125.

Rerole AL, Jego G, Garrido C. 2011. Hsp70: anti-apoptotic and tumorigenic protein. *Methods Mol. Biol.* **787**: 205–230.

Sanchez VC, Jachak A, Hurt RH, Kane AB. 2012. Biological interactions of graphene-family nanomaterials: an interdisciplinary review. *Chem. Res. Toxicol.* **25**: 15–34.

Shim G, Kim JY, Han J, Chung SW, Lee S, Byun Y, Oh YK. 2014. Reduced graphene oxide nanosheets coated with an anti-angiogenic anticancer low-molecular-weight heparin derivative for delivery of anticancer drugs. *J. Control Release* **189**: 80–89.

Singh M, Odeniyi DT, Apostolov EO, Savenka A, Fite T, Wangila GW, Walker RB, Basnakian AG. 2013. Protective effect of zinc-N-acetylcysteine on the rat kidney during cold storage. *Am. J. Physiol. Renal Physiol.* **305**: F1022–F1030.

Tian F, Cui D, Schwarz H, Estrada GG, Kobayashi H. 2006. Cytotoxicity of single-wall carbon nanotubes on human fibroblasts. *Toxicol. in Vitro* **20**: 1202–1212.

Wilczek P, Major R, Lipinska L, Lackner J, Mzyk A. 2015. Thrombogenicity and biocompatibility studies of reduced graphene oxide modified acellular pulmonary valve tissue. *Mater. Sci. Eng. C Mater. Biol. Appl.* **53**: 310–321.

Yang K, Li Y, Tan X, Peng R, Liu Z. 2013. Behavior and toxicity of graphene and its functionalized derivatives in biological systems. *Small* **9**: 1492–1503.

Yin X, Apostolov EO, Shah SV, Wang X, Bogdanov KV, Buzder T, Stewart AG, Basnakian AG. 2007. Induction of renal endonuclease G by cisplatin is reduced in DNase I-deficient mice. *J. Am. Soc. Nephrol.* **18**: 2544–2553.

Zhang Y, Ali SF, Dervishi E, Xu Y, Li Z, Casciano D, Biris AS. 2010. Cytotoxicity effects of graphene and single-wall carbon nanotubes in neural phaeochromocytoma-derived PC12 cells. *ACS Nano* **4**: 3181–3186.

Supporting information

Additional Supporting Information may be found online in the supporting information tab for this article.